CrystEngComm

Accepted Manuscript

ROYAL SOCIETY OF CHEMISTRY

www.rsc.org/crystengcomm

Crystallization of HPHT diamond crystals in a floatage system under the influence of nitrogen and hydrogen simultaneously

Guofeng Huang[1*], Youjin Zheng [2], Lizhi Peng[2], Zhanchang Li[1], Xiaopeng Jia[3] and Hongan Ma[3]

[1] Inor Mongolia Key Lab of High-pressure Phase Functional Materials, Chifeng University, Chifeng 024000, PR China;

[2] Lab of Superhard Materials, Mudanjiang Normal College, Mudanjiang 157011, PR China

[3] National Key Lab of Superhard Materials, Jilin University, Changchun 130012, PR China;

Abstract: Employing floatage as a driving force for diamond growth, crystallization of diamond crystals in Fe–Cr–C system co-doped with nitrogen and hydrogen elements is established at a static pressure of ~6.5 GPa and a temperature range of 1335–1485 ℃. Under the influence of nitrogen and hydrogen incorporated into diamond structure, simultaneously, a rich morphological diversity of diamond specimens is produced, such as hexagonal slice-shape, trapezoidal slice-shape, strip shape and triangular slice-shape crystals. Observation on infrared spectra from as-grown crystals indicates that a dramatic enhancement of the incorporation of hydrogen and nitrogen atoms with each other into diamond structure are present in strip-shape specimens, confirmed by a fact that a relatively high absorption coefficients at the peaks of 1130 cm^{-1}, and 1344 cm^{-1} accompany with high absorption coefficients at the bands of 2850 cm^{-1}, and 2920 cm^{-1}. Hydrogen-related absorption in three-phonon region further indicated that hydrogen atoms existed in diamond structure in sp^3 bonded $–CH_2–$, and $–CH_3$ group form, respectively. At atmospheric pressure, these hydrogen-related structures are rather stable and can sustain high temperature up to 1800 ℃. Nitrogen donors are universally observed as isolated substitutional form in crystals, while minor paired-form nitrogen atoms readily formed in the strip shape crystals or other crystals crystallized at higher temperature.

Keywords: high pressure and high temperature, co-doping, annealing treatment, floatage growth process

*Corresponding author.
E-mail address：hgfsyn0925@163.com (G. Huang).

1. Introduction

Although, diamond posses an abundance of ultimate performance, it principally behaves as abrasive material universally applied in processing industry. In fact, the application field of diamond materials depends upon its properties and morphologies. In order to produce the desired and controlled properties from diamond material, the considerable research works have been, therefore, devoted to investigating the influence of minor elements (such as B, N, H, P, S, O, Ni, and Si) on diamond properties and crystallization behaviors.[1–10] Of those chemical species that can be incorporated in sufficient concentrations, the more conspicuously successful doping is boron, either by chemical vapor deposition (CVD) process or by high pressure and high temperature (HPHT) process. The deliberate B-doping into diamond material can produce a *p*-type semiconductor, and can also yield metallic properties and superconductivity properties.[11] Using simple N-doping technique, *n*-type semiconductor diamond materials have been indeed produced, but it is of little value due to a deep donor level.[12] Even so, nitrogen still has significant potential in varying diamond properties, especially co-doping together with other impurities. In the case of hydrogen-doping, there is an evidence that a small fraction of hydrogen atoms have been taken up into the CVD diamond material, typically resulting from substantial hydrogen-containing species in the growth mixture.[13,14] However, it has been experimentally shown that hydrogen atom was rare detected in as-grown diamond crystal that crystallized in the traditional metal-medium system at HPHT conditions. On the contrary, investigation on the infrared (IR) spectra from natural diamonds has ever revealed that hydrogen atoms always accompanying with nitrogen impurities were commonly present in the natural type-Ia diamond stones.[15] In attempt to synthesis diamond containing both N and H, simultaneously, relevant experiments are initially performed at a low pressure of 5.3 GPa, demonstrating that the presence of melamine ($C_3N_6H_6$) leads to no nucleation.[16] Recent research works demonstrated that hydrogen-contained diamond could be grown in the metal medium doped with hydrogen-contained compounds.[17] Sun et. al. even suggested that a synergism effect

had played a role in the incorporation of H and N atoms into diamond structure.[18] It is a pity that an idea doping effect has not ever been achieved in their work. Nevertheless, at some appropriate conditions, the co-doping technique in varying the properties of as-grown diamond is still more effective in comparison to the simple doping, e. g. co-doping of HPHT diamond with B together with H atom does give rise to extremely promising electrical features.[19] To get further insight into the co-doping effect (N, H) on diamond properties and growth behavior, the addition of $C_3N_6H_6$ is, therefore, selected to act as the doping source.

Nowadays, CVD method has indeed achieved a major breakthrough in the production of single crystal diamond; nonetheless the majority of diamonds applied in processing industry are predominantly produced by the catalytic process with metal mediums at HPHT conditions.[20-22] Gem-quality diamond crystals are prepared by temperature gradient growth (TGG) process, in which temperature gradient acts as a driving force.[2,3,5] The diamond grits are produced by film growth (FG) process, in which graphite is transformed to diamond through a molten layer consisting of transition metals such as iron, cobalt and nickel. In this method, the driving force for the formation of diamond is derived from the difference in thermodynamic stability between two phases of carbon. Diamond grits, produced by this process, are of 0.3–0.6 mm in size within run duration of 15–30 minutes.[23] In our work, a new growth process, in which carbon atoms diffuse from carbon source to the crystallized sites in metal melt with floatage as a primarily driving force, is employed to control the growth rate in order to obtain high-quality diamond specimens. Considering that Ni and Co metal are readily trapped in diamond lattice, $Fe_{95}Cr_5$ is employed as the crystallization medium.

2. Experimental

The experiments on diamond growth were performed in a cubic anvil HPHT apparatus (SPD-8 × 1400). The assembly for the synthesis of diamond crystals by a floatage growth process was designed as presented in Fig. 1. The sub-heater was only added in the top side to avoid the presence of temperature gradient in metal solvent. The synthesis chamber was constructed by ceramic material, ZrO_2+MgO, with an

inner size of 13 mm in diameter. The highest pressure generated from this apparatus could reach ~7 GPa, estimated by the curve based on the pressure-induced phase transitions of Bi, Tl, and Ba. The collected diamond crystals were crystallized under a pressure of ~6.5 GPa and temperatures of ~1335–1485 °C. The temperature gradient between the carbon source and the seed bed was still present with extremely low value of less than 10 °C. The temperature was estimated from a correlation between the temperature and input power, which was calibrated using a Pt6%Rh–Pt30%Rh thermocouple. As for the annealing treatment, the argon gas is utilized to protect the diamond grains from graphitization. The annealing treatment was conducted in a stable temperature range of 1700–1800 °C, which is derived from the thermocouple of same type being used to in-situ measurement at atmospheric pressure within 0.5 h.

High-purity graphite was utilized as the carbon source, and the solvent-metal of $Fe_{95}Cr_5$ (95/5, weight ratio) was employed as the catalyst medium. The additive $C_3N_6H_6$ (99.99% purity) was mixed with the graphite powder (99.99% purity) and was pressed into a cylindrical sample as the initial material accommodated into the ampoule. The added amount of dopant $C_3N_6H_6$ varies from 0 to 1.5 wt.% compared with the mass of carbon source. After the HPHT synthesis with run duration of 7 h, the collected crude samples were first treated with dilute nitric acid to separate the diamond grains from the metal-catalyst medium. The diamond crystals were subsequently refluxed in the strong acid solution to eliminate the residual impurities present on the crystal surface. The as-synthesized diamond crystals free from bulk inclusions were selected for analysis by an optical microscope. Nitrogen and hydrogen in these diamonds were characterized by IR spectra recorded from Fourier transform infrared (FTIR) spectrometer in a spectral range of 500–4000 cm^{-1} with a resolution of 2 cm^{-1} in a transmittance mode. During the IR measurements, a Bomem M110 FTIR spectrometer fitted with a microscope was employed. The IR beam size was rescaled to the range of 50–150 μm in diameter for analyzing the absorptions only occurring in the diamond crystal. The single substitutional form (C-form) and aggregated form (A-form) nitrogen concentrations are estimated by absorption coefficients of 1130 cm^{-1} and 1282 cm^{-1}, respectively, with conversion factor of 25

and 16.5. Morphology and structural properties of the as-synthesized samples were characterized by scanning electron microscope (SEM) and powder X-ray diffraction (XRD). In the XRD test, X-rays with a setting wavelength of 1.54 Å are impinged upon samples, and the diffracted X-rays are detected at 2θ, the angle between the X-ray source and the detector.

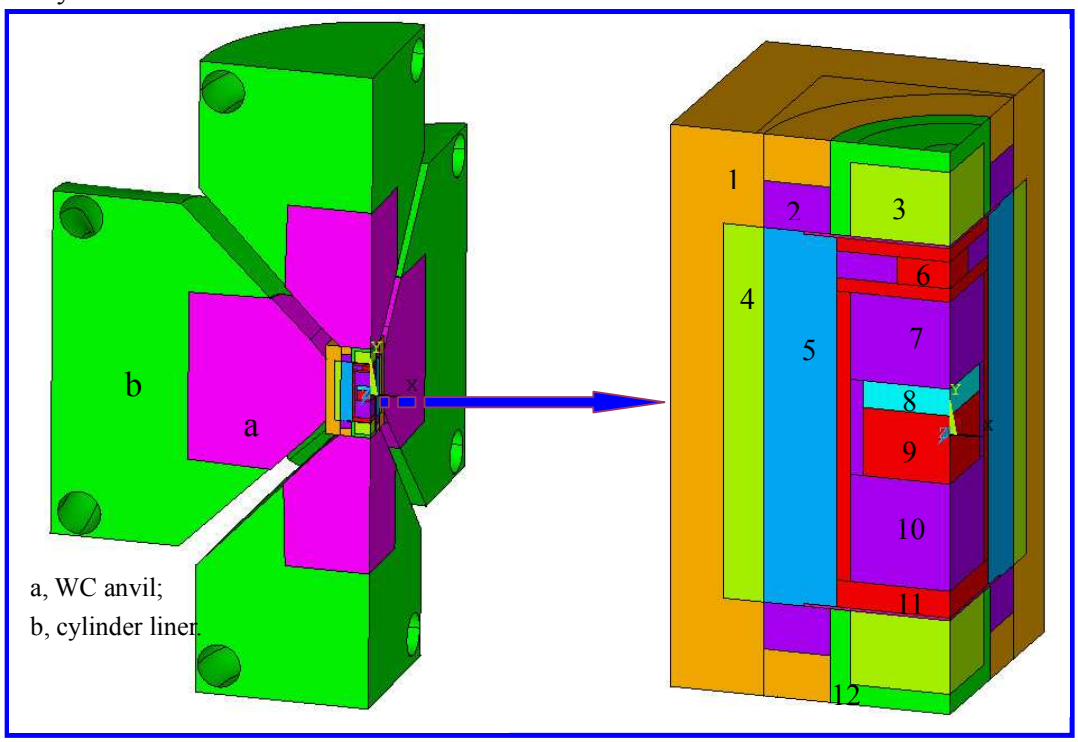

Fig. 1. Samples assembly of 1/4 part for diamond synthesis by HPHT: 1, pyrophyllite; 2, ZrO_2 sleeve; 3, end cap of dolomite; 4, dolomite sleeve; 5, $NaCl+Al_2O_3$ sleeve; 6, sub-heat of graphite; 7,10, cap of ZrO_2; 8, metal medium; 9, graphite of carbon source; 11, sheet graphite; 12, steel ring.

3. Results and discussion

The diamond crystallization under the influence of nitrogen and hydrogen elements is established in the Fe–Cr–C system at the HPHT conditions, as summarized in table 1. At the temperature range 1335–1485 °C, crystals nearly colorless in color, spontaneously nucleate and grow without deliberate doping. The morphology of crystals is predominantly octahedral with only {111} faces as a result of the special property of metal melt. Crystal morphology was primarily affected by temperature and the content of melamine doped into the growth cell. As the doping content of 0.5 wt.% was added, diamond crystallized mainly in the form of slice shape consisting of

Table 1. Experimental results and the characteristics of obtained crystals

Run	T/°C	Additive content/wt.%	obtained diamond crystals		
			Size /mm	Morphology	color
N-1	1335	0	0.5–0.8	octahedron	nearly colorless
N-2	1335	0.5	0.4–1.0	octahedron, slice of hexagon	dark yellow
N-3	1385	0.5	0.5–2.5	slice of trapezoid, and strip	yellow
N-4	1435	0.5	0.5–2.1	slice of triangle, and strip	light yellow
N-5	1385	1.0	0.4–2.8	slice of trapezoid, triangle and strip	light yellow
N-6	1435	1.0	0.5–2.4	slice of triangle, and strip	light yellow
N-7	1485	1.0	0.5–1.6	slice of triangle, and strip	light yellow
N-8	1435	1.5	0.5–3.4	slice of triangle, and strip	light yellow
N-9	1485	1.5	0.5–2.8	slice of triangle, and strip	light yellow

two large hexagons in the parallel faces at a low temperature of 1335 °C, as illustrated in Fig. 2a. Meanwhile, a relatively small fraction of octahedral-shape crystals, which is the same as that grown by FG process, are also produced, and the typical image is shown in Fig. 2b. With the temperature increasing from 1385 °C to 1435 °C, a slice shape of trapezoid (Fig. 2c) evolves into a slice shape of triangle (Fig. 2e), and the strip shape crystals always accompany, as displayed in Fig. 2 (f, h). It is worthy of mentioning that specimens, regardless of shape, readily have considerable macro-defects resembling serration locating the rims of surface, as depicted in Fig. 2 (d, g). A reason to cause this phenomenon may be attributed to the poor wettability of the FeCr metal-solvent, which is generally associated to the viscosity of melt metals. With increasing the doping content to 1.0 wt.%, there is a drastic change in diamond crystallization processes and three types of morphologies, slice of trapezoid, slice of triangle and strip, form simultaneously. The optical images of the involved typical crystals are presented in Fig 3. At a temperature beyond 1435 °C, the coexistence of

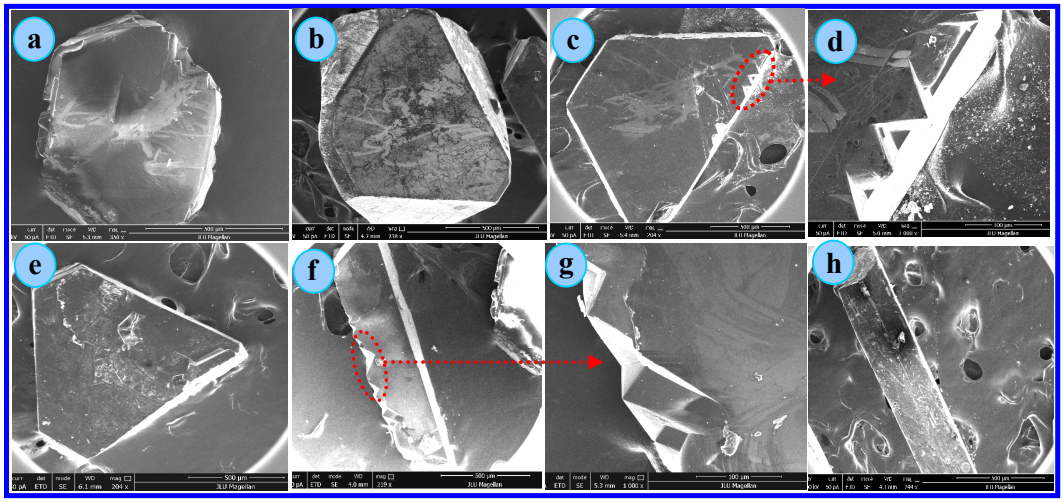

Fig. 2. SEM images of specimens grown by the floatage growth process at doping content of 0.5 wt.%: (a, b) 1335 °C, (c, d, f , g) 1385 °C, (e, h) 1435°C.

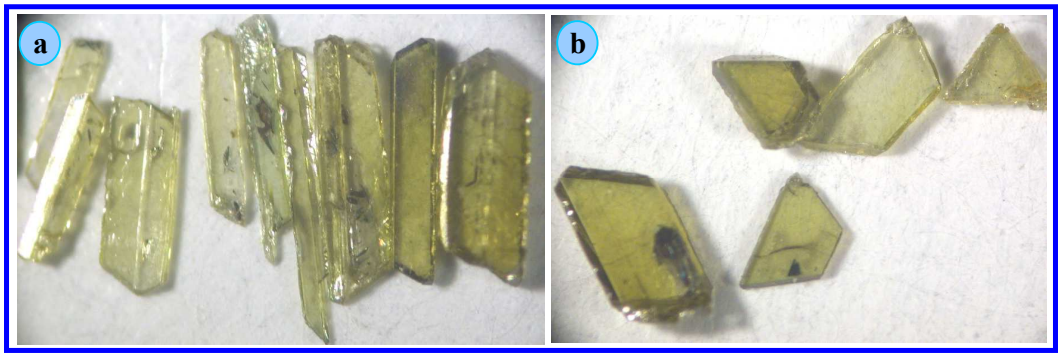

Fig. 3. Optical images of diamond crystals with (a) strip shape and (b) slice of triangle and trapezoid shape.

two types of morphologies, slice of triangle and strip, is universally observed. In the temperature range of 1385–1485 °C, there is a various trend of differing-shape crystals in product yield. The proportional production of strip-shape crystals decrease with crystallized temperature rising but increases with doping content of additives. On the contrary, the quantity of slice shape crystals has an inverse trend with temperature and the doping amount of additions. With further increasing doping content of additive to 1.5 wt.%, crystal growth region markedly narrows to the range of 1435–1485 °C, and the collected crystals are nearly unchanged in morphology and color; nevertheless, apart from diamond phase, the metastable graphite phase also forms and some can even be incorporated into diamond structure, indicated by the

XRD as illustrated in Fig. 4. Furthermore, the additional experiments carried out at higher temperature exceeding 1485 °C demonstrate that the floating carbon source from carbon source crystallizes only as a graphite phase, even though this phenomenon is forbidden in thermodynamic theory.

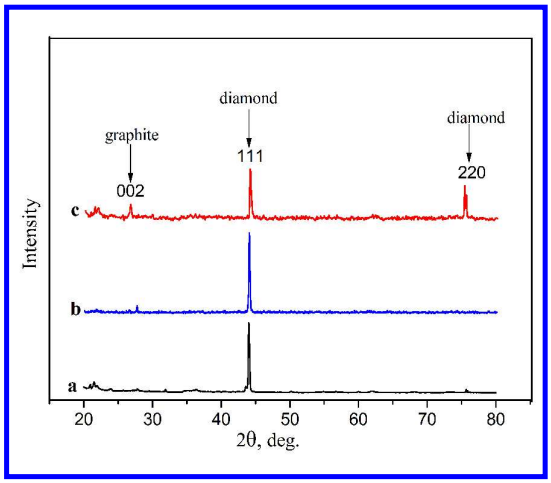

Fig. 4. Powder XRD of obtained diamond samples from (a) N-4, (b) N-8, (c) N-9.

It can be noted that a diversity of crystal morphologies have been produced. The experimental data regarding diamond crystallization in the Fe–Cr–C system in the presence of $C_3N_6H_6$ additives, obtained in this study, allow us to consider the formation mechanism of each type of crystal morphology under the influence of N and H incorporated into diamond network simultaneously. As is known, nitrogen impurity added in growth medium can be used to the controlling synthesis of strip-shape diamond crystal. The composition segregation in crystal growth metallic film is suggested by M. H. Hu. et. al.[24] This explanation seems not reasonable, in that, carbon and nitrogen atoms can be well dissolved and transported in the metal melt. Based on the current concept on crystal growth, it may be assumed that nitrogen arranged in diamond lattice varying the surface character, and some growing planes favor to accommodate the diffusing carbon atoms and some planes are not active to combine with new carbon atoms. Certainly, it is still an unsolved problem with respect to the detailed mechanism of nitrogen element affecting the developing crystal planes. In this study, slice shape and strip shape crystals were collected, especially

doping with higher content of melamine. The slice-shape diamond may be primarily attributed to the effect of hydrogen. It has ever been observed that the adsorption of impurities drops the specific surface energy of crystals which are cultivated from solutions, melts or a gas phase. Noting that each carbon atom in the growing facets of { 111 } has one uncompensated bond, it can not catch new carbon atom to continue development where absorption of hydrogen atoms takes place, irrespective of what form of them to enter specimen, and therefore the crystal planes heavily doped by hydrogen atoms with a low specific surface energy eventually survive. Accordingly, it may be suggested that the random discrepancy of growing facets in adsorbing hydrogen impurities results in the rich diversity of crystal morphologies. Based on the consideration above, we can infer that there are two planes severely suppressed by the adsorbing hydrogen impurities, and consequently slice-shape diamonds eventually form. As for the strip-shape crystals, nitrogen and hydrogen impurities simultaneously play a significant role acting as depression elements to prohibit four planes developing. Based on the analysis above, the previous described result with respect to the variation of quantity of strip-shape and slice-shape crystals can be interpreted. The decrease of production of strip shape crystals with crystallized temperature increasing is induced by lower depression effect of impurities (N, H) at higher temperature condition, and consequently the quantity of slice-shape crystals deservedly increase. Certainly, with doping content increasing, a proportion of the impurities which play a depression role will be sufficiently adsorbed in the developing surface, leading to a higher product yield of strip-shape crystals and a lower production of slice-shape crystals.

According to the inference concerning the formation mechanism of crystal shape upon melamine doping, the crystals in different morphologies should contain differing concentration of impurities. Consequently, the as-grown crystals were categorized into three types to be detected by means of FTIR spectroscopy in order to analyze the configuration and concentration of the incorporated nitrogen and hydrogen in crystals. The typical IR spectra from octahedral crystals are displayed in Fig. 5. It can be observed that the active absorption bands in the IR spectrum correlated with

hydrogen atoms locate around 2850 cm^{-1} and 2920 cm^{-1} (Fig. 5b), which are indicative of symmetric and asymmetric stretch vibration of sp^3 bonded $–CH_2–$ group. As for diamonds in this shape, the noticeable hydrogen atoms incorporated into diamond lattice depresses the absorption of nitrogen atoms. It can be found that nitrogen atoms exist in octahedral-shape crystals merely as C-form, indicated by the

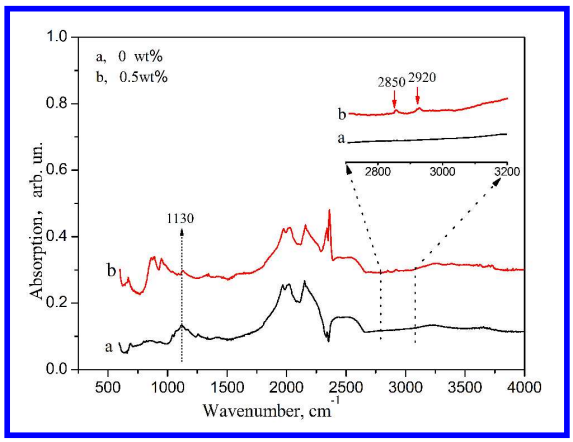

Fig. 5. Typical IR spectra recorded for octahedral-shape diamond crystals grown in Fe–Cr–C system with different adding content of $C_3N_6H_6$: (a) without additive (N-1); (b) 0.5wt.% (N-2).

presence of absorption peaks at 1130 cm^{-1} and 1344 cm^{-1}. As for slice-shape crystals, with the doping content of $C_3N_6H_6$ increased from 0.5 wt.% to 1.5 wt.%, the hydrogen-related absorption peaks (2850 cm^{-1} and 2920 cm^{-1}) in three-phonon region progressively get intense as displayed in Fig. 6. The paired form nitrogen atoms

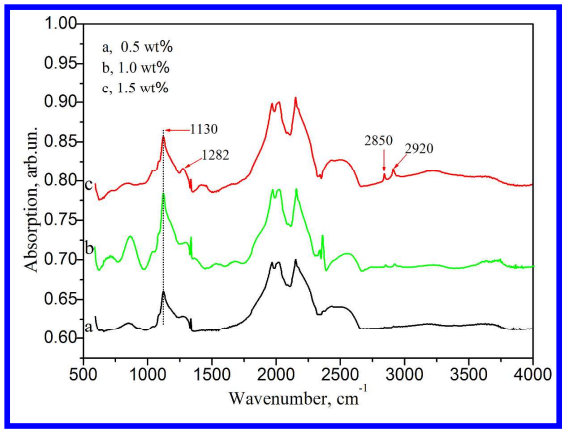

Fig. 6. Typical IR spectra recorded for slice-shape diamond crystals produced at various adding content of melamine and temperature conditions: (a) 0.5 wt.%; (b) 1.0 wt.%; (c) 1.5wt.%.

characterized by the absorption peak of 1282 cm^{-1} start to form at crystals grown at

1435 °C and 1.5 wt.% doping. The IR spectra (Fig. 7) derived from strip-shape crystals with nearly the same thickness demonstrate that an increase in additive $C_3N_6H_6$ content induces an enhancement of nitrogen-related absorption at 1130 cm^{-1} and 1282 cm^{-1}, which indicates an increase in nitrogen concentration of C-form and A-form. Meanwhile, absorption bands of 2850 cm^{-1} and 2920 cm^{-1} also have an appreciably enhanced trend. Furthermore, the hydrogen-related absorption peaks are dramatically intense in the spectrum from a strip-shape crystal than that from a slice shape or octahedral shape crystal even at the same doping condition.

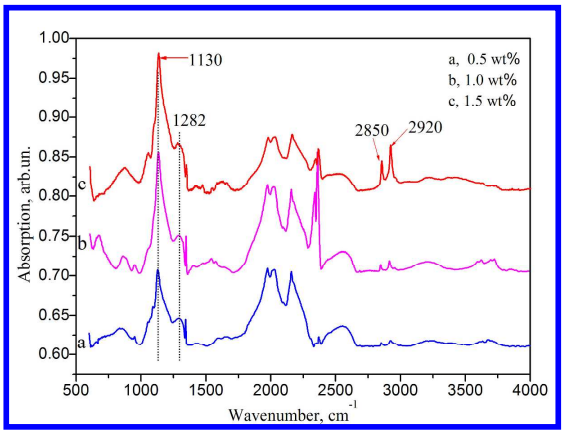

Fig. 7. Typical IR spectra recorded for strip-shape diamond crystals produced at various adding content of melamine and temperature conditions: (a) 0.5 wt.%; (b) 1.0 wt.%; (c) 1.5 wt.%.

In order to closely observe C–H stretch vibration region, the typical IR spectrum in three-phonon region from strip-shape crystal is presented in Fig. 8 after fitted with Gaussian peaks. It can be observed that the more intense absorption band appears at 2920 cm^{-1} comparing with that of 2850 cm^{-1}, indicating that a large proportion of hydrogen atoms exist in a form of sp^3 bonded asymmetric $–CH_2–$ group. Additionally, the absorption bands located 2960 cm^{-1} and 2890 cm^{-1} are fitted out in C–H stretch vibration region, respectively, which are due to the asymmetric and symmetric stretch vibration of a group of sp^3 bonded $–CH_3$. This fitted result shows a little discrepancy in adsorption from the symmetric stretch vibration of $–CH_3$ groups, which generally occurs at 2880 cm^{-1} in H-doping CVD diamond films. It should point out that the vibration of C–H bonds in $N–CH_3$ and $O–CH_3$ groups, the structures of which were generally detected in H-doping CVD diamond films, were, however, undetected in the

collected crystals.

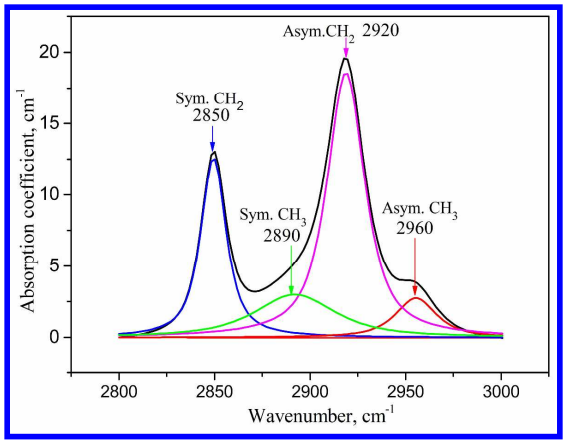

Fig. 8. Typical IR spectra in C–H stretch region (2800–3000 cm^{-1}) recorded from specimen (N-8) with stripe shape.

To examine the stability of H-related structures, atmospheric annealing treatment on strip-shape specimens is performed with argon air protecting specimens from graphitization. The results demonstrated that the as-synthesized specimens would severely graphitize at temperatures beyond 1900 °C, and the hydrogen-related structures of $–CH_2–$ and $–CH_3$ were rather stable in crystals at temperatures below 1800 °C (Fig. 9). As the presence of H in diamond lattice has serious repercussion for its characteristics, the quantitative estimation of hydrogen bonded to diamond

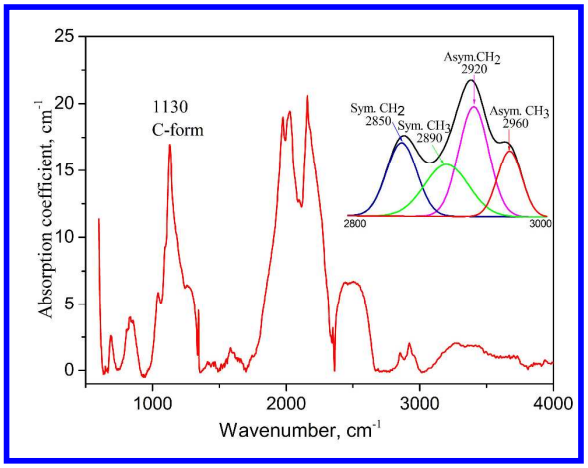

Fig. 9. Typical IR spectra recorded from a strip-shape diamond specimen (N-3) after atmospheric annealing treatment at a temperature of 1800 °C within 0.5 h (the insert showing C–H stretch vibration region).

lattice is rather difficult. Therefore, Table 2 only presents calculation results on

nitrogen concentrations in various shape crystals. Observation on variation of absorption coefficients relative to hydrogen structure and nitrogen concentrations shown in table 2 reveals that nitrogen and hydrogen atoms are favorite to be incorporated into crystal lattice at lower temperature at the same doping condition, and the concentrations of nitrogen and hydrogen depend upon crystal shape, indicating that the capability of growing crystals in adsorbing impurities follows an obvious sequence: strip shape > slice shape > octahedral shape. Noting that a noticeable nitrogen atoms (30–64 ppm), in A-form, are present in strip-shape crystals in a temperature range of l385–1485 °C which has not arrived at thermal dynamic conditions of nitrogen aggregation, it can be interpreted that the incorporation of hydrogen atoms decreases the activation energy of nitrogen aggregation.

Table 2. Impurity concentrations in specimens estimated from IR spectra with uncertainty of 5–10 %.

Shape	Added Melamine/ wt.%	Tem./ °C	Nitrogen concentration		
			N_A/ppm	N_C/ppm	N_T/ppm
octahedron	0	1335	0	87–122	87–122
octahedron	0.5	1335	0	14–57	14–57
slice	0.5	1335	0	92–112	92–112
strip	0.5	1385	35-40	275–291	310-331
slice	1.0	1385	0	307–332	307-332
slice	1.5	1435	25-30	254–289	279-319
strip	1.0	1385	30–43	373–405	403–448
strip	1.0	1435	43–56	287–357	330–413
strip	1.5	1435	81–92	524–749	605–841
strip	1.5	1485	53–64	409–512	462–576

Apparently, H atoms have been sufficiently doped into diamond structures. The successful doping should ascribe to the floatage acting as a driving force, which is largely different from FM process or TGG process, as illustrated in Fig. 10. In this

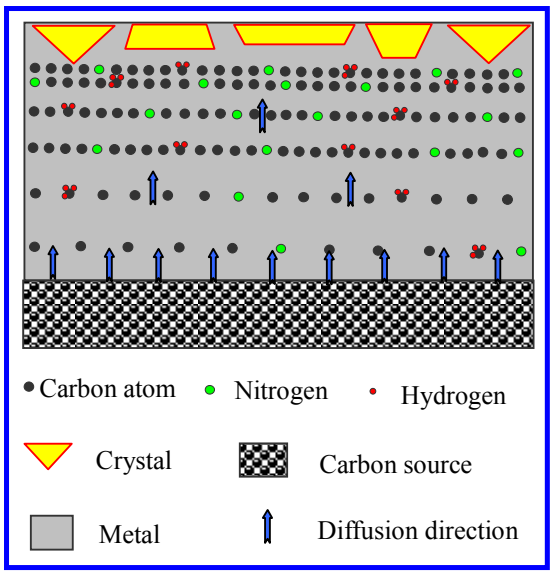

Fig.10. Schematic diagram to illustrate the diffusion mechanism of carbon atoms and impurities in a floatage system.

process, impurities readily condense at the top side of metal solvent; even can diffuse from the area of low concentration of impurity to that of high concentration, assisted by Archimedes buoyancy of impurities in solvent. On the contrary, in traditional process (FM or TGG), the transport of impurities essentially depends on gradient of impurity concentration, and consequently impurities can only diffuse from the area of high concentration to that of low concentration. It is this special diffusion mechanism of impurity that contributes the success in the heavy hydrogen-doping on diamond specimens.

It is generally accepted that the absorptions of 3107 cm^{-1} and 1405 cm^{-1} in IR spectrum, which characterize C–H stretching vibration mode and bending vibration mode, respectively, result from vinylidene group, $>C=CH_2$, in sp^2 bonding form, generally existing in type-Ia natural diamond crystals.[25] However, this structure is undetectable in the collected samples. Instead, the sp^3 bonded $–CH_2–$ and $–CH_3$ groups appear in as-synthesized crystals confirmed by IR spectra. It is of interest to consider in which form of hydrogen and nitrogen are incorporated into crystal structures during the growth process. The fact that abundant nitrogen atoms enter crystal lattice in C-form confirms that nitrogen element decomposed from organics of $C_3N_6H_6$ is trapped in crystal networks as an individually atomic form rather than a

group form. Detection of no nitrogen-related group in IR spectra, such as N-CH_3 group, also supports this viewpoint. Considering the presence of hydrogen element in a form of –CH_2– group accompanied by a small fraction of –CH_3 groups in crystal structure, it seems reasonable to assume that hydrogen atoms are trapped into crystal in a group form during crystal growth process, such as –CH_2–, and –CH_3 groups. As reported, high resolution X-ray photoelectron spectroscopy has confirmed that, in hydrogen atmosphere, the hydrogen-related structures, including monohydride, dihydride, and trihydride, are sufficiently formed on the diamond surface.[26,27] The same form of hydrogen in –CH_2– group is also detectable in diamond specimens synthesized with the addition of LiH, TiH, and $C_{10}H_{10}Fe$ acting as the dopant source, respectively.[8,9,17] Nevertheless, diamond crystals crystallized at temperatures of 1700–1900 °C with Fe_3N as catalyst medium unintentionally contaminated by NH_3, hydrogen impurities in a group form of >C=CH_2 characterized by 3107-cm^{-1} absorption can be widely observed.[7] Annealing experiments on natural diamond stones which have not active absorption corresponding to hydrogen atoms in IR spectra have indicated a convinced result that hydrogen in >C=CH_2 form can be produced after HPHT annealing treatment at T=2650 °C, P=9 GPa.[28] Taking the results above into account, one can confirm that hydrogen atoms enter diamond structure as a group form, for individual hydrogen atoms are undetected in specimens. Moreover, the occurrence form of hydrogen depends upon temperature condition of crystal growth process. This consideration is supported by an experimental fact that –CH_2– group presents in diamond specimens synthesized in the NiFe–C–H_2O system in the temperature range 1300–1370 °C, while the structure of >C=CH_2 appears instead in diamond crystals grown in the S–C–H_2O system at temperatures exceeding 1800 °C.[29,30] It should mention that the groups of –CH_2– and –CH_3 have not ever been detected in natural diamond stones until now, but the structure of >C=CH_2 is universally observed in natural diamond stones of type-Ia. This result leads us to consider that the formation of structure of >C=CH_2 may be evolved from –CH_2– group upon annealing treatment at extremely high pressure and high temperature. Referring the research works of pioneers, it can be concluded that the groups of

–CH_2– and –CH_3 are formed in a low temperature range 1300–1500 °C and can steadily exist in crystals at atmospheric pressure and high temperatures up to 1800°C; the steady structure of >C=CH_2, probably stemming from –CH_2– group, generally appears in diamond specimen at growing temperatures beyond 1700 °C.

4. Conclusion

At a pressure of 6.5 GPa and temperatures of 1335–1485 °C, diamond crystals crystallized in Fe–Cr–C system co-doped with hydrogen and nitrogen impurities by a floatage growth process were explored. A diversity of crystals, octahedral shape, slice shape, and strip shape in morphology were produced, due to the absorption of hydrogen and nitrogen donors into crystal structure. The nitrogen and hydrogen atoms are favored to be incorporated into crystals at low temperature conditions, and the obviously higher concentrations of nitrogen and hydrogen occur in strip shape crystals. Nitrogen high up to 749 ppm primarily in C-form appears in co-doped diamond crystals accompanied by a small fraction of A-form nitrogen atoms at the level of a few tens of ppm. It can be confirmed that nitrogen atoms enter diamond structure in an individually atomic form, and hydrogen atoms are incorporated into crystal lattice as a group form of –CH_2– and –CH_3.

Acknowledgements

This work was financial supported by the Natural Science Foundation of Inner Mongolia (Grant No. 2013MS0809), the Scientific Research Program of Inner Mongolia (Grant No. NJZC13308), and the Open Project of State Key Laboratory of Superhard Materials of Jilin University (Grant No. 201310).

References

1. V. S. Bormashov, S. A. Tarelkin, S. G. Buga, M. S. Kuznetsov, S. A. Terentiev, A. N. Semenov, V. D. Blank, Diamond Relat. Mater., 2013,35,19–23.
2. V.D. Blank, M.S. Kuznetsov, S.A. Nosukhin, S.A. Terentiev and V.N. Denisov, Diamond Relat. Mater., 2007, 16, 800–804.

3. Y. N. Palyanov, Y. M. Borzdov, A. F. Khokhryakov, I. N. Kupriyanov and A. G. Sokol, Cryst. Growth Des., 2010, 10, 3169–3175.
4. Z. Z. Liang, H. Kanda, X. Jai, H. A. Ma, P. W. Zhu,Q. F. Guan and C. Y. Zang, Carbon, 2006, 44, 913–917.
5. Y. Zhang, C. Zang, H. Ma, Z. Liang, L. Zhou, S. Li and X. Jia, Diamond Relat. Mater., 2008, 17, 209–211.
6. R. Z. Yu, H. A. Ma, Z. Z. Liang, W. Q. Liu, Y. J. Zheng and X. Jia, Diamond Relat. Mater., 2008, 17, 180–184.
7. Y. Borzdov, Y. Pal'yanov, I. Kupriyanov, V. Gusev, A. Khokhryakov, A. Sokol and A. Efremov, Diamond Relat.Mater., 2002, 11, 1863–1870.
8. Y. Li, X. P. Jia, M. H. Hu, X. B. Liu, B. M. Yan, Z. X. Zhou, Z. F. Zhang and H. A. Ma, Chin. Phys. B, 2012, 21, 058101.
9. Z. F. Zhang, X. P. Jia, S. S. Sun, X. B. Liu, Y. Li, B. M. Yan and H. A. Ma, Int. J. Refract. Met. Hard Mater., 2013, 38, 111–117.
10. X. B. Liu, X. P. Jia, Z. F. Zhang, Y. Li, M. H. Hu, Z. X. Zhou and H. A. Ma, Cryst. Growth Des., 2011, 11, 3844–3849.
11. E. A. Ekimov, V. A. Sidorov, E. D. Bauer, N. N. Mel'nik, N. J. Curro, J. D. Thompson, and S. M. Stishov, Nature, 2004, 428, 542–545.
12. Rafi Kalish, Journal of physics D: Applied Physics, 2007, 40, 6467–6478.
13. E. Titus, D.S. Misra, A.K. Sikder, P.K. Tyagi, M.K. Singh, Abha Misra, N. Ali, G. Cabral, V.F. Neto, J. Gracio, Diamond and Related Materials, 2005, 14, 476– 481.
14. E. Titus, N. Ali, G. Cabral, J.C. Madaleno, V.F. Neto, J. Gracio, P Ramesh Babu, A.K. Sikder, T.I. Okpalugo, D.S. Misra, Diamond and Related Materials, 2006, 515, 201–206.
15. Filip De Weerdt, Igor N. Kupriyanov. Diamond and Related Materials, 2002, 11, 714–715.
16. Z.Z. Liang, X. Jia, C.Y. Zang, P.W. Zhu, H.A. Ma, G.Z. Ren, Diamond and Related Materials, 2005, 14, 243–247.
17. Shishuai Sun, Xiaopeng Jia, Bingmin Yan, Fangbiao Wang, Ning Chen, Yadong Li and Hong-an Ma, CrystEngComm, 2014, 16, 2290–2297.

18. Shishuai Sun, Xiaopeng Jia, Bingmin Yan, FangbiaoWang, Yadong Li, Ning Chen, Hong-an Ma. Diamond and Related Materials, 2014, 42, 21–27.
19. Yong Li, Xiaopeng Jia, Hong-an Ma, Jie Zhang, Fangbiao Wang, Ning Chen and Yunguang Feng, CrystEngComm, 2014, 16, 7547–7551.
20. Bert Willems, Alexandre Tallaire, Jocelyn Achard, Diamond and Related Materials, 2014, 41, 25–33.
21. Alexandre Tallaire, Jocelyn Achard, François Silva, Ovidiu Brinza, Alix Gicquel, Comptes Rendus Physique, 2013, 14, 169–184.
22. L. Zhou, X. Jia, H. Ma, Y. Zheng, and Y. Li, Chinese Physics B, 2008, 17, 4665–4668.
23. N.D. Zhigadlo, Journal of Crystal Growth, 2014, 395, 1–4.
24. M.H. Hu, H.A. Ma, W.Q. Liu, Z.F. Zhang, M. Zhao, Y. Li, W. Guo, J.M. Qin, X. Jia, 2010, 312, 2989–2992.
25. G. S. Woods, A. T. Collins, J. Phys. Chem. Solids, 1983, 44, 471–475.
26. S. Ghodbane, F. Omnes, C. Agnes, Diamond and Related Materials, 2010, 19, 273–278.
27. X. Wang, A. R. Ruslinda, Y. Ishiyama, Y. Ishii, H. Kawarada, Diamond and Related Materials, 2011, 20, 1319–1324.
28. I. Kiflawi, D. Fisher, H. Kanda, G. Sittas, Diamond and Related Materials, 1996, 5, 1516–1518.
29. Yuri N. Palyanov, Alexander F. Khokhryakov, Yuri M. Borzdov, and Igor N. Kupriyanov, Crystal Growth and Design, 2013, 13, 5411–5419.
30. Y. N. Palyanov, I. N. Kupriyanov, Y. M. Borzdov, A. G. Sokol, and A. F. Khokhryakov, Crystal Growth and Design, 2009, 9, 2922–2926.

Optical images of strip-shape diamond crystals grown by a floatage system with FeCr acted as solvent-metal